Applied Energy 394 (2025) 126124

Contents lists available at ScienceDirect

Applied Energy

journal homepage: www.elsevier.com/locate/apen

Energy management for modular proton exchange membrane water electrolyzers under fluctuating solar inputs: a constrained nonlinear optimization approach

Ashkan Makhsoos[a, b,*], Mohsen Kandidayeni[a], Meziane Ait Ziane[c], Mohammadreza Moghadari[a], Loïc Boulon[a], Bruno G. Pollet[a, b]

[a] Hydrogen Research Institute (HRI), Department of Electrical Engineering and Computer Science, Université du Québec á Trois-Rivières (UQTR), 3351 boulevard des Forges, Trois-Rivières, Québec, G9A 5H7, Canada

[b] GreenH2Lab, Hydrogen Research Institute (HRI), Department of Chemistry, Biochemistry and Physics, Université du Québec á Trois-Rivières (UQTR), 3351 boulevard des Forges, Trois-Rivières, Québec, G9A 5H7, Canada

[c] Université de Lorraine, GREEN, Nancy, F-54000, France

HIGHLIGHTS

- Novel nonlinear EMS enhances PEM electrolyzer efficiency under solar variability.
- Rotary allocation strategy reduces degradation and ensures balanced stack use.
- Validated electrochemical model optimized using genetic algorithms.
- EMS achieves highest annual hydrogen yield and efficiency among benchmarks.

GRAPHICAL ABSTRACT

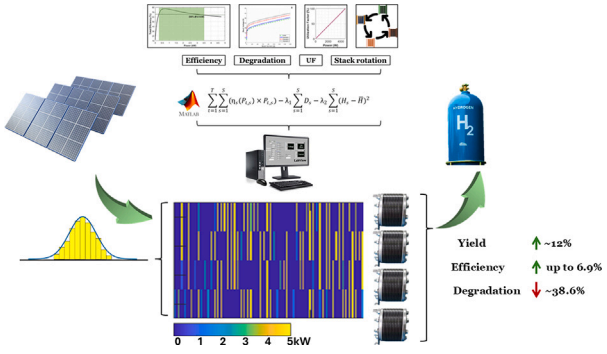

ARTICLE INFO

Keywords:
Energy management
PEM electrolyzer
Renewable energy
Nonlinear optimization
Rotary power allocation
Solar energy integration

ABSTRACT

This study introduces an advanced nonlinear optimization-based energy management system (EMS) specifically designed for modular Proton Exchange Membrane Water Electrolyzers (PEMWE) under fluctuating solar energy conditions. To optimize system efficiency, reduce degradation, and maintain balanced stack operation, the Rotary Power Allocation Strategy (RPAS) employs a dynamic power distribution method that allocates power among multiple stacks based on current demand. A validated electrochemical model calibrated through laboratory experiments and genetic algorithm optimization serves as the foundation for the analysis. Benchmarking in this study has demonstrated the superiority of the proposed strategy to established EMS methods, such as rule-based, fuzzy logic, composite optimization, and decentralized multi-agent scheduling. In terms of system efficiency, it has been demonstrated that there is an increase of 63 % in system efficiency, a greater hydrogen yield exceeding 4200 kg per year, and a considerable reduction in stack voltage degradation. The strategy effectively addresses key limitations associated with conventional EMS approaches, ensuring consistent and equitable stack usage, thus providing a robust, scalable solution for renewable energy-driven hydrogen production.

* Corresponding author at: Hydrogen Research Institute (HRI), Department of Electrical Engineering and Computer Science, Université du Québec á Trois-Rivières (UQTR), 3351 boulevard des Forges, Trois-Rivières, Québec, G9A 5H7, Canada
Email address: ashkan.makhsoos@uqtr.ca (A. Makhsoos).

https://doi.org/10.1016/j.apenergy.2025.126124
Received 10 April 2025; Received in revised form 9 May 2025; Accepted 13 May 2025
Available online 23 May 2025

1. Introduction

Energy management is crucial to minimizing energy consumption in all sectors, as illustrated in Fig. 1, to reduce expenditures, improve efficiency, and reduce environmental impact. Its applications span a variety of industries, such as manufacturing, data centers, and Renewable Energy Sources (RESs), and it involves implementing energy-saving measures and monitoring energy in real-time [1]. In numerous scenarios, including Heating, Ventilation, and Air Conditioning (HVAC) control in commercial buildings [2], manufacturing production efficiency [3], and data center electrical usage monitoring, Energy Management Systems (EMS) optimize operations, enhance sustainability, and save costs. For greater power efficiency, data centers, for instance, use sophisticated server management and cooling systems [4].

In addition to facilitating RES integration, EMS ensures consistent energy distribution while resolving intermittency issues. By combining Hydrogen Production (HyPro) with the availability of renewable energy, EMS optimizes the production, storage, and distribution of hydrogen [5]. When coupled with fuel cell systems, EMS-enabled smart grids can improve grid efficiency by dynamically adjusting load to reduce transmission losses and enhance the integration of renewable energy. For example, modifications to wind turbines and optimized solar panels can improve grid efficiency further when coordinated with fuel cell systems [6]. Day-ahead scheduling and scenario clustering are innovative strategies that boost energy utilization and improve the economic viability of HyPro systems. For example, in [7] the authors introduced a multi-state transition electrolyzer model integrated with energy storage to clearly demonstrate these benefits. While EMS oversees hydrogen fueling stations to satisfy the needs of fuel-cell vehicles, electrolyzers dynamically modify operations for sustainability and cost-effectiveness. In a comparable way, authors of [8] enhance energy efficiency and lower costs in renewable-rich settings by using demand response mechanisms in microgrids.

According to recent research, EMS has improved the efficiency, longevity, and grid stability of electrolyzers in hydrogen systems during HyPro operations [9]. To support its function as a scalable renewable energy vector, EMS also tackles issues with hydrogen transportation and storage [10].

PEMWE technology has advanced recently due to its compatibility with intermittent Renewable Energy Resources (RESs) such as solar and wind. PEMWE is a flexible, zero-emission energy storage system that solves intermittency problems and improves grid stability by effectively converting surplus renewable energy into hydrogen with rapid response times [11]. Market research indicates that the PEMWE industry will develop rapidly as governments and businesses embrace hydrogen as a crucial component of the energy revolution [12]. Europe, Japan, South Korea, and the Middle East are making significant investments in hydrogen initiatives, highlighting the relevance of PEMWE in integrating RESs to achieve carbon neutrality [13]. Membrane, catalyst, and system design technological advancements have lowered PEMWE costs, increasing its economic feasibility and competition with conventional techniques. The development of efficient electrocatalysts and robust ion exchange membranes is essential if performance is to be improved and operating costs to be reduced [14]. Because modular PEMWE systems are flexible and scalable, they can be adapted to integrate with local renewable projects and respond dynamically to changing energy sources [15]. Modularity increases hydrogen generation efficiency while meeting industrial automation standards.

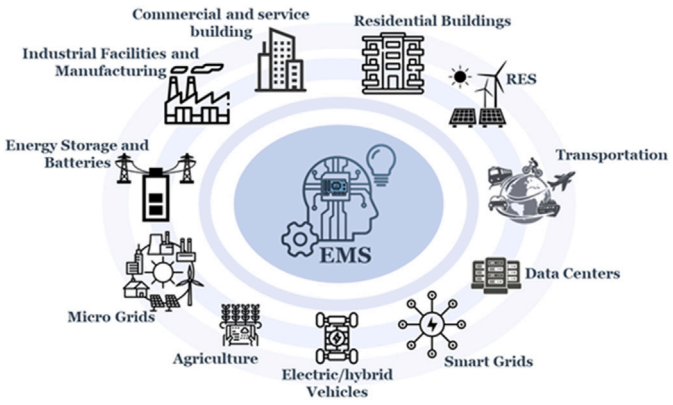

Fig. 1. Utilizations of EMS.

For scalable, high-capacity electrolysis systems, [16] stress the shift from monolithic to modular designs, while authors of [17] emphasize the use of modern materials and machine learning for their selection in order to increase the durability and efficiency of electrolyzers. Authors in [18] highlight how High-Temperature Electrolysis (HTE) devices show commercial feasibility. To optimize alkaline electrolysis stacks in variable renewable conditions, authors of [19] provide quantitative model that considers interrelated factors (electrode size, position and number), which increase performance by more than 6 %. They have done it by decreasing the bubble coverage effect and shunt current effect.

From single-module configurations for places that are limited to scalable modules that guarantee continuity under variable energy supplies, PEMWE systems are made to be operationally flexible. These systems support a low-carbon economy by adjusting to the availability of renewable energy. It is still difficult to successfully integrate RESs because of high upfront costs and the requirement for efficient EMSs.

To maximize PEMWE energy utilization, effective energy management is critical, directly impacting both capital expenditures (CAPEX) and operational expenditures (OPEX) of modular systems. A modular system consists of a number of subsystems, including cooling, gas separation, power supply, and water treatment (see Fig. 2). PEMWE stacks account for approximately 70–85 % of total energy consumption, followed by gas handling at 10–15 %, and cooling systems consuming around 4–10 % as illustrated in Fig. 3. As a result, an optimized EMS can greatly enhance efficiency and cost-effectiveness by minimizing unnecessary cycling of subsystems and extending stack lifecycle [20].

Strategies for integrating wind energy with hydrogen generation are highlighted in [15,21]. The design and operation of PEMWE and alkaline electrolyzers optimized in [22] using a multi-scale, multi-period mixed-integer linear programming method to maximize economic viability. The model enhances HyPro through cost-effective supply chain solutions by integrating strategic (plant locations, capacities) and operational (process scheduling, raw material flows) decisions, while also accounting for uncertainties (feedstock availability, hydrogen demand, etc.). Chandrasekar examines wind curtailment for PEMWE and Solid Oxide Electrolysis Cells (SOEC), highlighting the efficiency disparity between low- and high-temperature electrolyzers under fluctuating power. Authors of [23] use MATLAB/Simulink to study grid stability with wind-to-hydrogen systems to achieve reliable frequency stabilization.

Using genetic algorithms for solar-powered hydrogen synthesis, authors in [24] suggest incorporating Parabolic Trough Collector (PTC) and thermoelectric generators to enhance the efficiency and hydrogen yield of the system. While the work in [25] evaluates direct PV-electrolyzer connections for solar energy conversion in Iran, authors in [26] study PV-electrolyzer systems, highlighting efficiency fluctuations with environmental changes.

Authors of [27] develop a finite-state machine-based EMS for a solar-powered hydrogen unit, achieving 73 % electrolyzer efficiency and reliable operation. In their optimization of DC microgrids combining PEMWE, and in [28] place an intense focus on energy storage and the efficiency of hydrogen production.

Modular designs for operational flexibility are among the advancements in PEMWE scalability. Authors of [29] improve energy efficiency with interleaved DC-DC converters, while in [30] use neural networks to optimize geothermal hydrogen systems. Layered power scheduling is

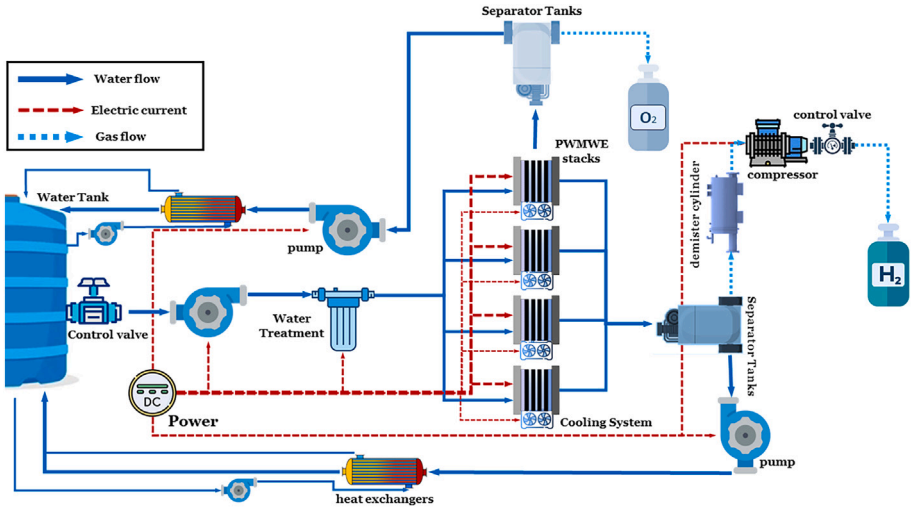

Fig. 2. Modular PEMWE system and subsystems.

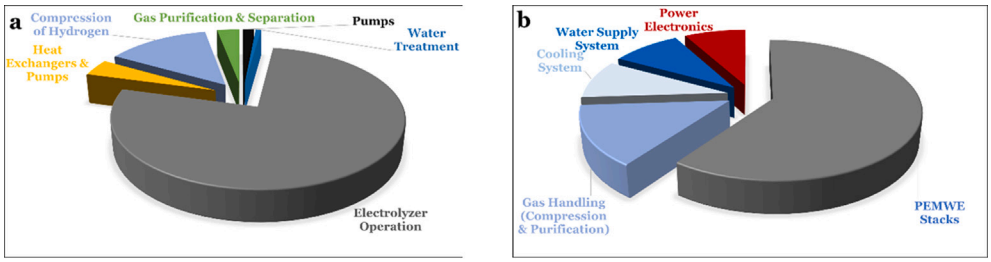

(a) Energy consumption (b) Costs breakdown in modular PEMWE systems

Fig. 3. Energy consumption and costs.

employed in [31] to minimize expenses and deterioration in PEMWE systems.

Grid flexibility is improved by attempts to integrate PEMWE with Virtual Power Plants (VPPs) and smart grids. PV-PEMWE systems have been improved in [32] using Particle Swarm Optimization (PSO), increasing efficiency in the presence of deterioration and shade.

Degradation in PEM water electrolyzers remains a critical challenge that directly impacts system longevity, efficiency, and operational costs. Under dynamic operation and high current density, voltage degradation is caused by numerous intertwined mechanisms, such as catalyst dissolution, membrane thinning, and PTL degradation. Empirical studies have reported voltage degradation rates ranging from a few microvolts per hour under steady-state conditions to tens of microvolts per hour in dynamic cycling, particularly in renewable energy-driven systems [33]. In particular, authors of [34] demonstrated that thermal cycling exacerbates the degradation of membrane performance, while in [35] identified significant fluoride emissions at elevated temperatures, indicating membrane degradation as the dominant failure mode. In addition, authors of [36] have demonstrated the impact of fluctuating power input on PTL oxidation and membrane stress, concluding that transient operations result in higher degradation rates than continuous ones. To address these challenges, researchers have developed degradation models ranging from empirical voltage-loss predictions to physics-based and machine-learning-enhanced approaches. Authors of [37] demonstrate that there is a trade-off between catalyst loading and degradation rate, demonstrating that lower Ir loadings, while cost-effective, can have a detrimental effect on performance. Similarly, authors of [38] conducted comprehensive diagnostics on material ageing, correlating membrane thinning with increased ohmic resistance and catalyst degradation with rising overpotential. The findings support the need for energy management strategies that mitigate degradation using load balancing, controlled ramp rates, and material innovations, which would ensure a lengthy electrolyzer lifetime suitable for large-scale hydrogen production.

The literature highlights several gaps concerning the optimization of EMS for modular PEMWE systems under fluctuating renewable energy inputs, specifically regarding efficiency optimization [33,34,36,39], degradation mitigation, and adaptive operational management [17]. Existing rule-based energy management methods often lead to inefficiencies [40], uneven stack utilization, and accelerated component degradation [22,30], particularly in situations when input conditions are extremely changeable [41]. Authors of [42,43] extensively reviewed modeling approaches focusing on control-oriented methodologies for realistic simulations and energy management applications. Similarly, in [44,45], authors offered important insights into dynamic modeling, experimental validation, and practical implementation issues, particularly highlighting degradation induced by power converter current ripple. Furthermore, in [4,46], authors examined system-level operational strategies for PEMWE systems with intermittent renewables, addressing integration challenges. Thus, a solid foundation was established for the understanding of how electrolyzer dynamics interact with renewable energy variability.

Focusing more specifically on modular multi-stack configurations, recent research has explored various strategies to optimize energy management and power allocation among PEMWE stacks. Because of persistent low load conditions, common strategies, such as equal current distribution, have been criticized for causing suboptimal operation and accelerated degradation [47]. Sequential allocation methods, on the

other hand, achieve higher efficiency but risk uneven stack degradation due to concentrated utilization [48]. By utilizing advanced adaptive strategies, such as those demonstrated in [49], power allocation can be dynamically adjusted in response to real-time performance metrics, improving efficiency by approximately 5–10 % from traditional approaches. A number of heuristic frameworks have been proposed in [50,51], along with optimization-based frameworks [52–54]. Several approaches have been presented to balance hydrogen production efficiency with degradation mitigation by balancing rotational loads and careful planning of operations.

Over the past five years the community has moved decisively beyond simple linear or sequential loading rules toward mathematically and data-driven energy-management schemes for multi-stack PEMWE. Centralized optimizers now dominate the state of the art: Mixed-Integer Linear Programs (MILP) schedule stack on/off states on an hourly basis while respecting cold and hot-start penalties and electricity-price signals [55]; rolling-horizon MPC formulations extend this concept to minute-level dispatch, continuously updating set-points as renewable forecasts change [56]. Parallel efforts embed explicit degradation terms–e.g., membrane-voltage rise per coulomb passed–directly into the objective so that power is steered toward stacks operating on the optimal-efficiency frontier while cumulative wear is minimized [52]. In contrast, several groups pursue lightweight but still adaptive heuristics: segment-start or First-In-First-Out rotation rules cut daily start–stop cycles by >40 % relative to fixed-priority control [57,58], whereas segmented fuzzy-logic allocators smooth the transition between partial-load and full-load regions and deliver 3–5 % higher specific hydrogen yield [53]. Finally, multi-agent architectures based on the module-type-package standard distribute the optimization burden among stack-level agents that negotiate power split via Alternating Direction Method of Multipliers (ADMM), achieving almost the same cost optimum as a MILP while offering superior fault tolerance and plug-and-play scalability [59]. Together, these studies establish a clear trajectory from rule-based control toward optimization- and agent-based strategies that explicitly balance efficiency, degradation and flexibility.

However, existing approaches remain limited despite these advancements. Most studies rely heavily on simplified or heuristic degradation models. Consequently, this simplification reduces the predictive accuracy and practical applicability of current management strategies [53,60]. However, in our study, various operational modes are considered to illustrate the variation in degradation by adopting literature-based models specifically developed for degradation analysis. Several adaptive and optimization-based strategies present computational challenges or are highly predictive, which makes their real-time implementation in practical industrial environments difficult. Using constrained nonlinear optimization techniques, this paper presents a novel, practically feasible Rotary Power Allocation Strategy (RPAS). The proposed approach dynamically balances power distribution to simultaneously enhance operational efficiency, effectively mitigate degradation, and extend stack lifespan, thereby distinctly advancing the state-of-the-art in modular PEMWE energy management.

As a result, the paper consists of the following sections: Section 2 provides a detailed model of the PEMWE. The test bench used for model validation is described in Section 2.2. The two case studies of energy management strategy are presented in Section 2.3. The suggested EMS framework and optimization strategy are presented in Section 3. In Section 4, comprehensive results, analyses and comparisons between the developed EMS and traditional rule-based strategies are presented, demonstrating significant improvements in hydrogen yield, efficiency, and reduced degradation rates. The conclusion is provided in Section 5.

2. PEMWE modeling and case studies

2.1. Electrochemical cell model

PEMWE cells use electrical energy to split water into hydrogen and oxygen. A PEMWE system's hierarchical structure, from setup to the molecular scale, is depicted in detail in Fig. 4. Initially, the diagram illustrates the system configuration, highlighting the power sources and control mechanisms, and demonstrating the modularity of the electrolyzer. In a cross-section, key components such as anode and cathode catalysts, membranes, porous transport layers (PTLs), flow channels and bipolar plates (BPPs) are visible. The figure demonstrates the proton transfer within the membrane by illustrating the movement of protons (H^+), hydrogen (H_2), oxygen (O_2), and water (H_2O) molecules, thereby explaining how hydrogen is produced through electrochemical reactions and electrical flow.

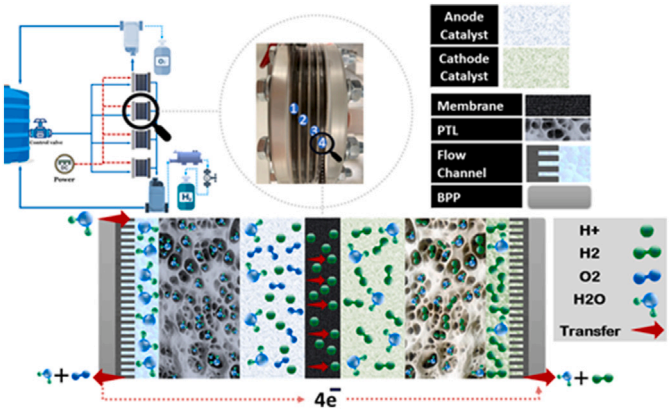

Fig. 4. Integrated overview of PEMWE system, stack, and cell components and proton transfer processes.

Three essential processes provide a concise description of the electrolysis of water in PEMWE cells. In reaction given in (1a) liquid H_2O is electrolyzed, resulting in the formation of O_2 gas, H^+ in aqueous solution, and electrons (e^-). In (1b) these H^+ and e^- recombine at the cathode to produce H_2 gas. These steps are combined to demonstrate the net conversion of liquid water into equal molar amounts of hydrogen and oxygen gases in the whole process, which is summed up in (1c) [61].

$$2H_2O \longrightarrow O_2 + 4H^+ + 4e^- \tag{1a}$$

$$4H^+ + 4e^- \longrightarrow 2H_2 \tag{1b}$$

$$2H_2O \longrightarrow O_2 + 2H_2 \tag{1c}$$

The efficiency and performance of a PEMWE depend significantly on the cell voltage (V_{cell}), which is a combination of the reversible voltage and various overpotential losses. The cell voltage is expressed by

$$V_{cell} = V_{rev} + U_a + U_o + U_c \tag{2}$$

where V_{rev} represents the minimum voltage required under ideal conditions to split water into hydrogen and oxygen. This voltage is derived from thermodynamic principles, specifically Gibbs free energy, and can be expressed by

$$V_{rev} = V_{rev,s} + \frac{RT}{2F} \times \ln\left(\frac{P_{H_2} P_{O_2}^{0.5}}{\alpha_{H_2O}}\right) \tag{3}$$

where the standard reversible voltage $V_{rev,s}$ is a temperature-dependent parameter, essential for electrochemical calculations and is expressed as follows

$$V_{rev,s} = 1.229 - 0.9 \times (T - 298) \times 10^{-3} \tag{4}$$

where T is temperature in Kelvin, R the universal gas constant $R = 8.314\,\mathrm{J/mol}$ and F the Faraday constant ($F = 96,485\,\mathrm{C/mol}$). The partial pressures of hydrogen and oxygen is expressed by P_{H_2} and P_{O_2},

Table 1
Test bench specifications.

Parameters	Specifications	BOP	Specifications
Model	QLC-1000	Temperature	5–35 °C
Number of cells N	4	Water/hydrogen pressure	101.325 Pa/4.905 kPa
Operational current range	0–36 A	Power supply	0–100 V, 0–100 A
Active area	50 cm^2	Control mechanism	PC-controlled power supply
Operational voltage range	DC 12–15 V	Data acquisition	myDAQ/Extech thermometer
Hydrogen production rate	1000 ml/min	H_2 flow control	Omega FH

respectively. The activity of water α_{H_2O} is typically assumed to be 1 in liquid-phase electrochemical calculations.

Activation overpotential U_a arises due to the energy barrier that must be overcome for electrochemical reactions to occur at the electrode surfaces, particularly the hydrogen evolution and oxygen evolution reactions. Using the well known Butler–Volmer equation, the activation overpotential U_a can be expressed by

$$U_{a,j} = \frac{RT}{\alpha_j z F} \sinh^{-1}\left(\frac{i_j}{2i_{0,j}}\right) \tag{5}$$

where j refers to anode or cathode side which the U_a will be their sum, α_j represents the fraction of the voltage that drives the electrochemical reaction. The number of electrons transferred z is typically 2 for water electrolysis, indicating the participation of electrons in the reaction. The current density at electrode i_j reflects the current per unit area at the electrode surface, while the exchange current density $i_{0,j}$ is a measure of reaction kinetics at equilibrium, indicating the rate of electron transfer without any net electrolysis. At low current densities, where reaction kinetics play a more significant role, activation overpotentials are one of the major contributors to cell voltage.

Ohmic losses U_o occur due to resistance to ion flow through the electrolyte and other cell components. A direct cause of these losses is the electrical resistance present in the PEMWE, including the proton-conducting membrane and the conductive materials used. The Ohmic losses can be expressed by

$$U_o = I \times \Omega_{eq} \tag{6}$$

where I is the current through the cell, Ω_{eq} is the equivalent resistance of the cell, which can be further broken down into the main resistances which are membrane Ω_M and electrodes Ω_E resistance. It is also common for researchers to consider multiple layers (PTL, CL and...) of ohmic resistance separately or to disregard some of them, but when a model is fitted automatically, most of the resistance will be considered. The equivalent resistance of the cell Ω_{eq} can be expressed as follows

$$\Omega_{eq} = \Omega_M + \Omega_E \tag{7}$$

The Ω_M depends on its thickness and conductivity, which in turn are functions of water content and temperature. The membrane resistance can be expressed as:

$$\Omega_M = \frac{\theta}{\mho} \tag{8}$$

where θ is the thickness of the membrane and $\mho$ is the membrane conductivity, which is a function of water content λ and temperature and is expressed by

$$\mho = (0.005139\lambda - 0.00326)\exp\left(1268 \times \left(\frac{1}{303} - \frac{1}{T}\right)\right) \tag{9}$$

Based on (9), it is shown that as the moisture content or temperature of the membrane increases, the membrane conductivity will improve, resulting in a reduction in ohmic losses.

Concentration overpotential U_c occurs when there is a difference between the concentration of reactants at the electrode surface and their concentrations in the bulk solution. This overpotential is particularly significant at higher current densities, where the supply of reactants becomes diffusion limited. The U_c can be calculated by

$$U_c = \frac{RT}{zF} \ln\left(\frac{i_l}{i_l - i}\right) \tag{10}$$

where i_l is the limiting current and determined by the diffusion capabilities of the system. This equation highlights how the overpotential increases as the operating current approaches the diffusion-limited current [62].

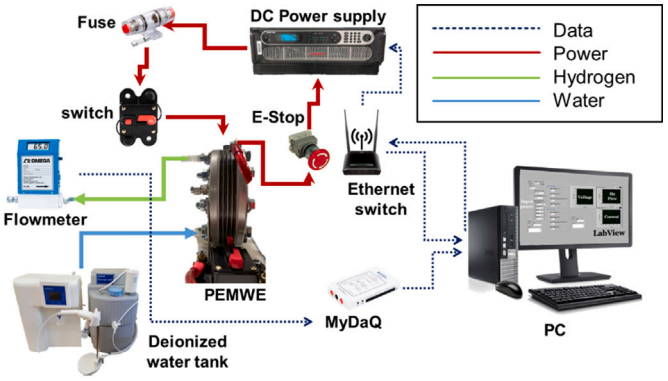

Fig. 5. Setup of the PEMWE test bench: instrumentation and control system configuration.

2.2. Test bench and model validation

An experimental test bench designed for PEMWE systems was used to validate this model, which is based on a benchmark developed by the team in previous research studies [63]. The test bench specifications are given in Table 1. The test bench facilitates accurate measurement of current, voltage, and gas flow rates, managed through National Instruments interfaced with LabVIEW, as shown in Fig. 5. The aluminum foil used as a current collector has a thickness ranging between 8–25 μm, aligning with common practices in PEM electrolyzer configurations. In accordance with typical values reported for such materials, the gas diffusion layer (GDL) consists of carbon cloth woven into a weave that has an uncompressed porosity of approximately 80–85 %. The system can produce hydrogen at a rate of 1000 ml/min and oxygen at a rate of 500 ml/min. As shown in Table 1, the QLC-1000 PEMWE system features four cells, each with an active area of 50 cm^2, operating within a current range of 0–36 A and a voltage range of DC 12–15 V.

The chosen model was tuned using experimental data from the test bench, employing a Genetic Algorithm (GA) to adjust the parameters, thus minimizing the error between the calculated and experimental polarization curves [63]. This GA-based tuning ensures that the model accurately reflects real-world performance, with the optimized parameters detailed in Table 2.

The polarization curve, illustrated in Fig. 6, represents the relationship between cell voltage and PEMFC current density. It serves as a crucial tool for assessing electrolyzer efficiency and performance across

Table 2
PEMWE single-cell model parameters.

Parameters	Amount	Unit
Universal gas constant (R)	8.314	J/(mol K)
Faraday's constant (F)	96,485	C/mol
Water activity α_{H_2O}	1	N/A
Exchange current density (i_0)	$1e^{-3}$	A/m^2
Limiting current density (i_l)	1.75	A/m^2
Temperature (T)	Variable	K
Pressure (P)	1.5	atm
Hydrogen pressure (P_{H_2})	1	atm
Oxygen pressure (O_2)	1	atm
Charge transfer coefficient (α)	1.54	N/A
Thickness of the membrane (θ)	285	μm
Electrolyte conductivity ($\eth$)	1	S/m
Membrane humidification (λ)	57	N/A
Ohmic resistance (Ω_M)	0.163	Ohms
Ohmic resistance (Ω_E)	0.054	Ohms
Stoichiometric coefficient (z)	2	N/A

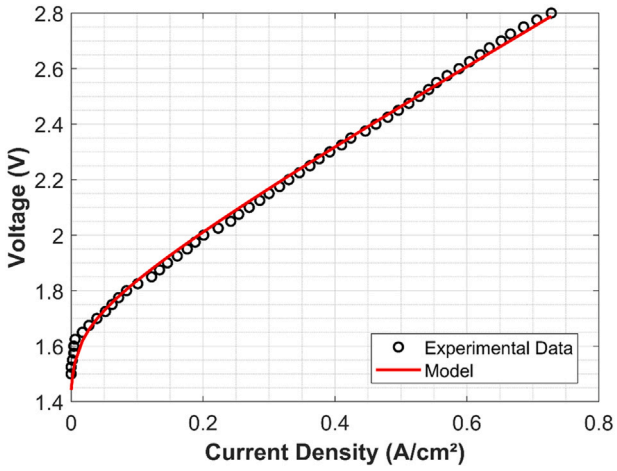

Fig. 6. PEMWE cell polarization curve.

various operational regions–highlighting activation losses at low current densities, ohmic losses at intermediate levels, and concentration losses at high densities. The experimental data for this curve are derived from measurements taken on the test bench, where the red curve indicates the tuned model and black curve represents the experimental data. It has been validated that the model fits well and is reliable for use in future calculations.

2.3. Case studies

This research investigates the performance and efficiency of a modular PEMWE under fluctuating solar inputs in Quebec, Canada. Two case studies are considered:

- **1st case study:** a 20 kW photovoltaic (PV) solar system located in Trois-Rivières was used as a renewable energy source to simulate real-world conditions. The PEMWE system consists of four modular 5 kW stacks. Data from PVWatts®version 8.4.0 [64] provided an estimations of solar power availability throughout a year, thus allowing a comprehensive evaluation of the EMS in balancing efficiency, degradation, and power allocation across stacks.
- **2nd case study:** is conducted using historical hourly generation data from the 80 MW Saddlebrook Solar facility, located in the South Planning Area of Alberta. This data, sourced from the Alberta Electric System Operator (AESO) [65], served as the input for simulating a scaled-up 80 kW PEMWE system composed of sixteen 5 kW stacks.

The main objective of these case studies is to validate a constrained nonlinear optimization approach and RPAS under realistic, variable operational scenarios.

Fig. 7 illustrates the standardized DC input power profile, for both case studies. Table 3 summarizes key technical specifications and performance metrics of the utilized PV system for the 1st case study. It is possible to evaluate the proposed EMS in terms of maintaining high operational efficiency and minimizing degradation under fluctuating solar input conditions thanks to these standardized gains.

The validated single-stack (0.5 kW) PEMWE model from the test bench is adapted for application in these case studies by scaling its parameters and operational characteristics to match the modular 5 kW stacks utilized. Adjustments include increasing the number of cells, active area, and operating current range to align with stack specifications. Using this method, it is possible to simulate stack performance under variable solar input conditions, thus bridging the gap between experimental validation and practical application. Building on the cell model described the relationship between a single cell and a single stack in the PEMWE is illustrated in (11). As shown in Table 4, the parameters for the 5 kW PEMWE discussed in this study were derived from both simulation results and parameters of existing commercial systems.

$$I_s = i \times A_a \tag{11a}$$
$$V_s = N \times V_{cell} \tag{11b}$$
$$P_s = I_s \times V_s \tag{11c}$$

The rate of HyPro based on Faraday's law can be described as follows

$$\dot{f}_{H_2} = \frac{N\,I\,RT}{2FP_{H_2}} \tag{12}$$

where, $\dot{f}_{H_2}$ is the HyPro flow rate in m^3/s, P_{H_2} denotes the partial pressure of hydrogen, expressed in atm [62].

3. Methodology, parameters and energy management

3.1. Efficiency

The voltage efficiency η_v of a PEMWE, representing membrane and heat losses, is calculated by assessing the cell voltage and it is determined by

$$\eta_v = \frac{V_{th}}{V_{cell}} \times 100 \tag{13}$$

where $V_{th} = 1.48$ V is the thermoneutral voltage [44].

The overall energy efficiency of the PEMWE system, denoted as η_s, is calculated by multiplying the individual efficiencies, as shown in (14a). This includes the voltage efficiency η_v and Faraday efficiency η_F, which accounts for losses due to gas diffusion. Although it is typically considered to be 1 [66], especially at standard operating pressures, it can be calculated using (14b) [67]. Additionally, Balance of Plant (BoP) efficiency η_{BOP}, which accounts for subsystems such as water and heat management, is assumed to range between 80 % and 100 % in literature [68,69]. In this study η_{BOP} is 90 %.

$$\eta_s = \eta_v \times \eta_F \times \eta_{BOP} \tag{14a}$$
$$\eta_F = (-0.0034P - 0.001711)i^{-1} + 1 \tag{14b}$$

Fig. 8 illustrates the total efficiency of the PEMWE system. As power increases, the overall efficiency reaches a peak before gradually declining due to increasing losses in the system.

3.2. Utilization factor

The utilization factor (UF) serves as a critical measure in efficient operation of a PEMWE stack, as it provides a clear indicator of how

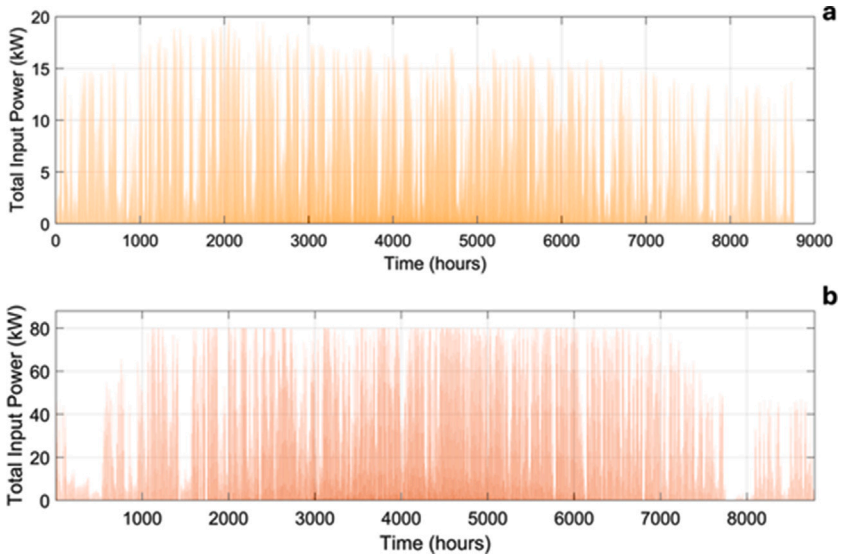

Fig. 7. Total input power: (a) 1st case study with 20 kW, (b) 2nd case study with 80 kW.

Table 3
PV system specifications, location and station identification: 1st case study.

Category	Specifications
Requested location	Trois-Rivieres
Weather data source	Lat, Lng: 46.35, −72.58 (0.7 mi)
Latitude	46.35° N
Longitude	72.58° W
DC system size	20 kW
Module type	Standard (Polycrystalline)
Array type	Fixed
System losses	14.08 %
Array tilt	66.5°
Array azimuth	185° (South-West)
Inverter efficiency	96 %
DC capacity factor	13.5 %

Table 4
Characteristics and parameters of the PEMWE stack.

Names	Parameters	Value	Unit
Rated power	P_s	5	kW
Operating voltage	V_s	15–28	V
Operating current	I_s	1–179	A
Cells number	N	10	N/A
Active area	A_a	248	cm^2
Operating pressure	P	196	kPa
Temperature	T	320	K

effectively the electrolyzer uses its capacity relative to its maximum potential of each stack. This evaluation helps in identifying operational efficiencies and areas for improvement. The stack utilization factor UF_s of a PEMWE is calculated as follows

$$UF_s = \frac{I_s V_s}{I_{\max} V_{\max}} \times 100 \tag{15}$$

where I_s and V_s are the in-use capacity and is the total power of the system and $I_{\max}$ and $V_{\max}$ represent the nominal current and voltage respectively, determined by the polarization curve. UF_s is expressed in percentage and reflects the system's power utilization efficiency. Fig. 9 illustrates a detailed analysis of the utilization factor for the PEMWE stack, demonstrating its performance across varying voltage, current, and power.

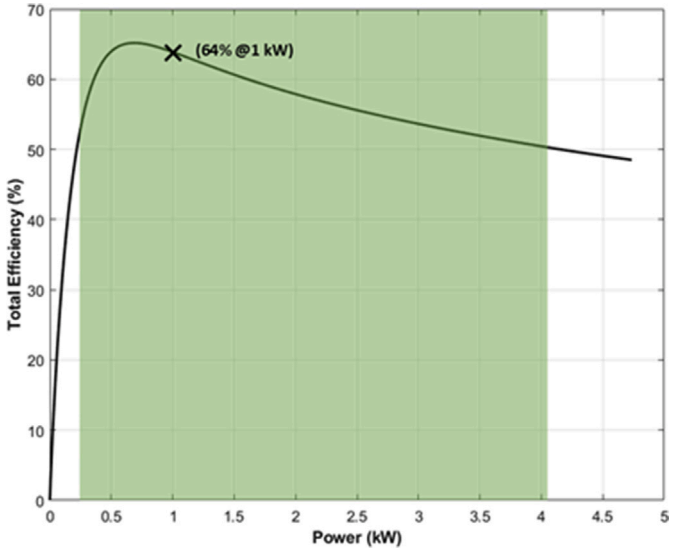

Fig. 8. Total efficiency vs. power curve of a PEMWE system.

3.3. Rotary power allocation strategy

Linear power allocation is a conventional, rule-based approach in modular PEMWE systems. Stack 1 is allocated power sequentially, and subsequent stacks are allocated power only when the previous stack reaches its maximum power capacity, as illustrated in Fig. 10 [70]. This often leads to uneven degradation and suboptimal system longevity. To address this, a Rotary Power Allocation Strategy (RPAS) is introduced, which dynamically distributes power across stacks in a cyclical manner.

RPAS dynamically distributes power among multiple stacks or modules, aiming to optimize operational efficiency and equipment longevity. RPAS, unlike linear allocation, avoids continuous stress on any single module by rotating power distribution systematically, which is more effective than linear allocation. By using this approach, degradation is significantly reduced, and overall system efficiency is enhanced, particularly when renewable energy inputs are variable.

RPAS primarily serves as a complementary strategy to the existing optimization system, ensuring correct activation and deactivation of stacks rather than introducing additional complexity to power

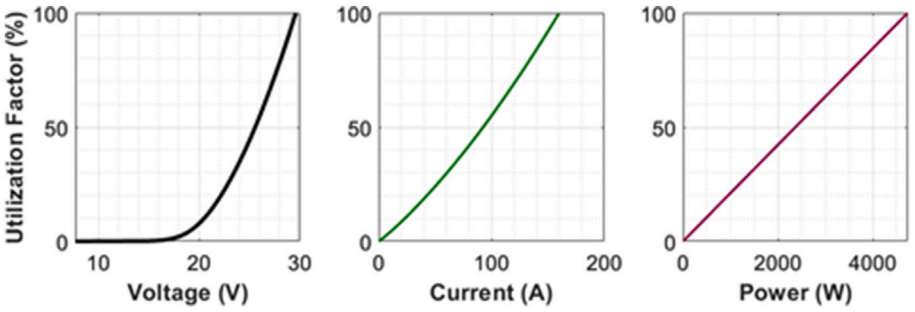

Fig. 9. Comprehensive utilization factor analysis of a PEMWE stack across voltage, current, and power dimensions.

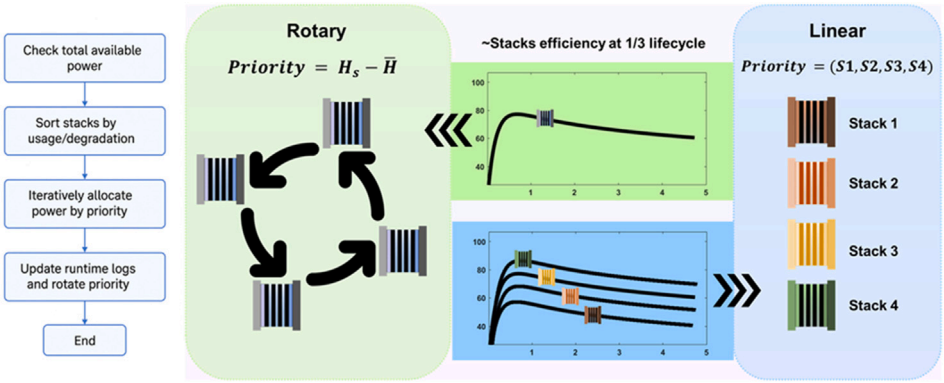

Fig. 10. Power allocation strategies.

allocation. It ensures the equitable use of all stacks and functions more as an insurance mechanism. Consequently, it improves system durability through a balanced load distribution, increases overall efficiency through optimization of stack usage, increases adaptability to fluctuations in power availability, and reduces maintenance frequency, which contributes to an increased system scalability.

3.4. Degradation and operational modes

The dynamic operation of a PEMWE stack is a significant factor driving component degradation, particularly affecting membranes, and catalysts. Membrane electrode assemblies (MEAs) are susceptible to chemical degradation mechanisms under dynamic operating conditions [71]. In particular, these phenomena are more pronounced during start-stop cycles and high-power operations in which fluctuations in voltage and current density lead to the degradation of in-situ layers that lead to increased voltage losses and reduced efficiency of the system. Key degradation processes include catalyst dissolution, membrane thinning, and ionomer degradation [72].

This degradation compromises operational efficiency by increasing the operating voltage of the PEMWE stacks as shown in Fig. 11. This degradation is quantified by analyzing voltage degradation rates to monitor the wear and ageing of the PEMWE components. Based on reports in the literature, the most significant degradation in PEMWE systems typically occurs during start-stop cycles, high-rated operations, and severe fluctuations. For example, high constant input power and frequent start-stop cycles accelerate the voltage degradation rate. This study assumes that the stack is fed smoothly and steadily, so only normal phase, stop-start and rated power operations are considered. Several studies, including [73], have thoroughly investigated these phenomena. Table 5 summarizes the average degradation observed in different operational modes in the literature, such as rated power [35], normal operation [67], and start-stop cycles which is an estimation based on existing data and the test bench operational conditions [74].

Table 5
Average degradation rates in PEMWE cell.

Operational mode	Average voltage degradation rate
Rated power	196 (μV/h)
Normal	35.5 (μV/h)
Start-stop cycling	60 (μV/cycle)

The progression of voltage increase due to degradation is illustrated in Fig. 11, which correlates increasing cell voltage with decreasing overall PEMWE efficiency. As the cell components wear down, the voltage required to maintain operation increases, thereby reducing the system's energy efficiency over time.

Understanding and quantifying the impacts of operational modes on PEMWE degradation are critical for extending the lifespan and optimizing the performance of these systems. The aggregate voltage degradation V_d in a PEMWE stack, factoring in each operational mode's contribution over time is expressed as follows

$$V_d = N\left(\delta V_R \times t_R + \delta V_n \times t_n + \delta V_{SSC} \times n_{SSC}\right) \tag{16}$$

where δV_R denotes voltage degradation during rated power operation, while δV_n refers to the same parameter in constant normal operation and parameter t stands for the time that each mode remains active in hours. The term δV_{SSC} indicates each start-stop cycle, and n_{SSC} represents the total number of such cycles experienced. N is the number of cells in the stack.

In a multi-stack system, each stack may experience a different operating schedule and therefore incur different degradation

$$D_s = N\left(\delta V_R \times t_R^{(s)} + \delta V_n \times t_n^{(s)} + \delta V_{SSC} \times n_{SSC}^{(s)}\right) \tag{17}$$

where $t_R^{(s)}$, and $t_n^{(s)}$ are the time stack (s) spends at rated and normal conditions. $n_{SSC}^{(s)}$ is the number of start–stop cycles that stack (s) undergoes.

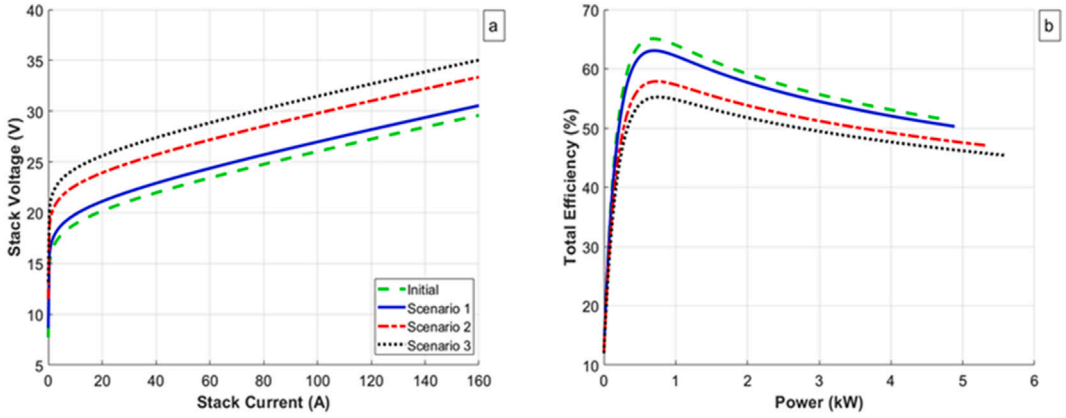

Fig. 11. Analysis of the effect of degradation on: (a) stack voltage (b) total efficiency of stack.

Fig. 11 illustrates three specific scenarios: in scenario 1, the 5 kW stack is subjected to a single start-stop cycle daily and operates in normal mode for 3000 h. Scenario 2 involves the same stack operating at rated power 70 % of the time, with one start-stop cycle daily included. Finally, scenario 3 entails continuous normal operation of the stack with start-stop cycles occurring every 6 h. These scenarios provide a comprehensive view of the stack's performance under different operational regimes.

3.5. Energy management strategy

The proposed EMS is based on a dynamic rotational strategy to optimize the allocation of power across multiple stacks, aiming to balance efficiency, degradation, and utilization effectively. There are priorities and weights for management in the following form:

1. **Maximizing total efficiency:** The power is distributed among stacks based on the highest efficiency at each moment, ensuring that stacks operate within their optimal efficiency range.
2. **Minimizing degradation:** Degradation is managed by minimizing rated power operation and start-stop cycles and distributing operational hours equally across stacks to avoid overloading any single unit.
3. **Balancing stack usage:** A rotational strategy ensures that all stacks are used evenly. This prevents the overuse of certain stacks while others remain underutilized, which can lead to uneven degradation.
4. **Adhering to UF constraints:** Stacks are only turned on when the available power is sufficient to meet the minimum UF thresholds, preventing unnecessary energy losses and degradation. Based on these objectives the optimization problem is formulated in (18) to maximize the efficiency while minimizing degradation and balancing stack utilization.

$$J = \sum_{t=0}^{T}\sum_{s=1}^{S}\left(\eta_s(P_{t,s}) \times P_{t,s} - \lambda_1 \sum_{s=1}^{S} D_s - \lambda_2 \sum_{s=1}^{S} (H_s - \bar{H})^2\right) \tag{18}$$

where $P_{t,s}$ is the power allocated to stack s at time t, $\eta_s(P_{t,s})$ stands for the efficiency of stack s based on the allocated power and D_s represents the degradation of stack s. Degradation penalty coefficient λ_1 controls the weight given to the degradation term in the objective function. The total operational hours of stack s is H_s, and $\bar{H}$ is the average operational hours across stacks. Balancing utilization penalty coefficient λ_2 ensures that the operational hours are balanced between the stacks. It penalizes situations where some stacks are overused compared to others. To provide operational flexibility across various use cases, the weight coefficients in (18) are designed to be adjustable. The degradation penalty coefficient λ_1 enables control over how strongly the optimizer penalizes degradation-heavy operations, while the utilization balancing weight λ_2 encourages uniform stack usage to prevent premature failure. These weights can be modified depending on external priorities such as minimizing maintenance, maximizing immediate hydrogen output, or adapting to electricity pricing dynamics. Tunability in the EMS allows it to operate in a variety of scenarios, including variable renewable energy supplies, differing load profiles, or specific economic constraints, achieving the optimal balance between performance and system health.

Several constraints are included in the model to ensure optimal performance, safety, and longevity of the system:

- **Stack capacity constraint:** each stack has a fixed maximum capacity ($P_{\max}$) of 5 kW. The power allocation to each stack must not exceed this limit to prevent overloading and potential damage, this constraint is defined as follows

$$\text{if } P_{t,s} \le P_{\max} \text{ than } con_c = 1 \tag{19}$$

- **Power allocation dynamics constraint:** ensures that the power allocated does not exceed the available power (P_{real}) from input power ($P_{t,s} \le P_{real}$).

$$\text{if } P_{t,s} \le P_{real} \text{ than } con_p = 1 \tag{20}$$

- UF **constraints:** a stack is only turned on if the allocated power as a percentage of its capacity is at least 20 %. This constraint ensures energy efficiency by avoiding operations under minimal load, which can be inefficient and lead to increased wear.

$$\begin{cases} \text{if } UF_{on} \le \dfrac{P_{t,s}}{P_{\max}} \text{ than } con_{F_{on}} = 1 \Rightarrow \text{turning on stack} \\ \text{if } UF_{off} \le \dfrac{P_{t,s}}{P_{\max}} \text{ than } con_{F_{off}} = 1 \Rightarrow \text{keeping a stack on} \end{cases} \tag{21}$$

where $UF_{on} = 0.2$ and $UF_{off} = 0.15$.

- **Stack rotation strategy constraint:** rotate operational duties among stacks to even out wear and tear, governed by $(H_s - \bar{H})$ and operational thresholds.

$$\begin{cases} H_s < \bar{H} \Rightarrow \text{turning on stack if} & con_c = con_p = con_{F_{on}} = 1 \\ H_s \ge \bar{H} \Rightarrow \text{keeping a stack on if} & con_{F_{off}} = 1 \\ H_s > \bar{H} \Rightarrow \text{turning off stack if} & con_c \ne 1 \text{ or } con_p \ne 1 \text{ or} \\ & con_{F_{on}} \ne 1 \text{ or } con_{F_{off}} \ne 1 \end{cases} \tag{22}$$

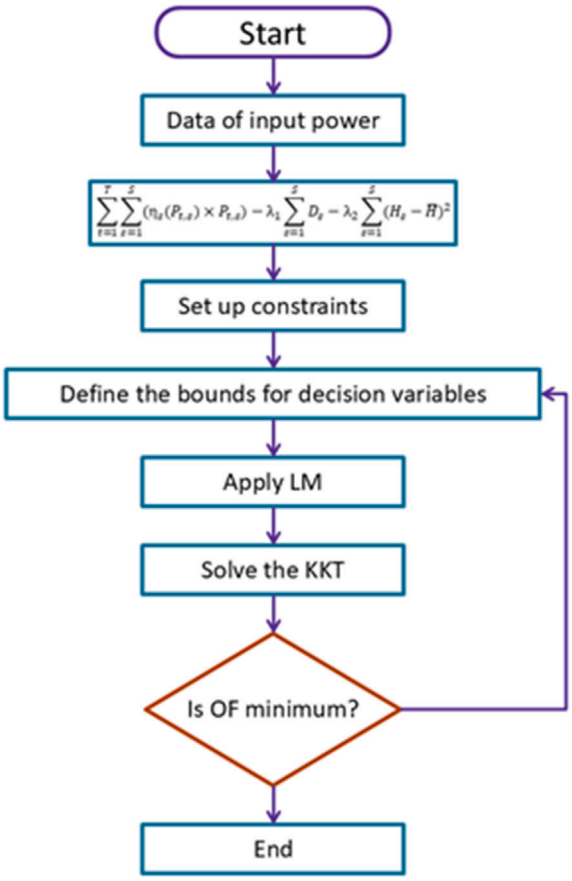

Fig. 12. Solution to the objective function.

These constraints are implemented using conditional logic within a loop over time and stack in the MATLAB code. Decisions to turn stacks on or off are based on the current power allocation relative to stack capacity and operational history, adjusting dynamically to changes in available power and operational needs. The actual efficiency and degradation computations adjust for current operating conditions using predefined mathematical formulas, ensuring the system operates within the defined constraints to optimize performance and longevity. This comprehensive approach integrates both operational and sustainability considerations, crucial for maintaining system efficiency and extending the service life of the PEMWE stacks.

3.5.1. Solving the objective function

Due to the inherent complexity and nonlinear characteristics of the system's operational parameters, nonlinear programming is chosen as the approach for solving the objective function for PEMWE system optimization. There are several nonlinear terms integrated into the objective function, including efficiency calculations, which entail exponential and logarithmic functions, particularly for modeling the activation, concentration, and ohmic overpotentials within the stack's electrochemical behavior. These overpotentials depend on the current density, itself a function of the power allocated to each stack, thus introducing nonlinearity. Furthermore, constraints like the minimum UF threshold introduce conditional behavior that linear programming cannot accommodate efficiently. In addition, nonlinear programming provides a robust and precise tool for maximizing operational efficiency while balancing degradation and ensuring equitable utilization across multiple stacks by incorporating these complex relationships and varying constraints into the optimization process.

The rationale for choosing nonlinear optimization over alternative techniques, such as linear programming or heuristic approaches, stems from the inherent complexities and accuracy requirements of the PEMWE system. Although linear programming is computationally simple, it is not capable of reproducing the nonlinear electrochemical relationships and operational dynamics involved, which could result in suboptimal or unrealistic solutions [75]. Meanwhile, heuristic methods, although often flexible, do not reliably ensure convergence to globally optimal solutions and typically lack theoretical optimality guarantees. Contrary to linear optimization, nonlinear optimization adheres to optimality criteria, in particular, the Karush–Kuhn–Tucker (KKT) conditions, which define the criteria for optimality [75].

At the optimal solution, the KKT conditions are satisfied via Lagrange Multipliers (LM), ensuring the solution's validity under the given constraints. As part of MATLAB's fmincon solver, the objective function and constraints are integrated into a Lagrangian function. It is then iteratively adjusted until convergence criteria (defined by gradient-based tolerances) are well achieved [76,77]. Consequently, solutions derived from this method are mathematically rigorous, reproducible, and robust.

A numerical method (e.g., finite difference approximations) is generally used to estimate the gradients of the nonlinear objective as well as the constraints within the solver. Additionally, line search or trust-region strategies regulate the step size, ensuring the solver maintains stability and robustness over the entire optimization horizon [78]. By integrating these numerical techniques, the nonlinear optimization solver navigates the complex landscape of constraints and nonlinear objective functions inherent to energy management in modular PEMWEs, particularly under fluctuating solar energy inputs.

This combined approach–encompassing nonlinear modeling, appropriate constraints, and rigorous numerical methods–is especially well-suited to addressing the dynamic and multi-dimensional challenges of modular PEMWE energy management. The entire solution process is illustrated in Fig. 12, showing how input data, constraints, and solver steps connect to find the optimal operating point for each stack.

4. Results

To evaluate the Proposed Strategy (PS), four selected state-of-the-art benchmark strategies covering a comprehensive range of current energy management paradigms (see Table 6). In [52] Efficiency–Degradation Composite Optimization (COMP) represents the forefront of optimization-based methods, employing a non-linear and mixed-integer formulation to simultaneously maximize instantaneous efficiency and minimize electrochemical ageing. In [79] a Segmented Fuzzy-Logic Allocator exemplifies modern heuristic methods, using a rule-based fuzzy control approach to dynamically adjust stack operations in real-time with minimal computational complexity. In [59] Decentralized Multi-Agent Scheduling (MAS) demonstrates the latest advances in distributed, agent-based scheduling, enabling modular stacks to independently optimize their performance through iterative negotiation and consensus algorithms. Finally, the Threshold-Based Rule (RB) EMS described by Fang and Liang [57] provides a conventional industrial benchmark, utilizing straightforward hysteresis-based logic to maintain each stack within efficient utilization bands, thereby minimizing frequent switching and wear. Collectively, these strategies span central optimization, adaptive heuristic control, distributed coordination, and traditional rule-based control, providing a balanced, transparent, and practically relevant basis for benchmarking RPAS using one-year solar dataset.

In the following, PS, COMP, Fuzzy, MAS and RB notations are used to designate the Proposed Strategy, Composite Optimization, Fuzzy logic, Multi-Agent Scheduling and Rule Based methods, respectively.

The efficiency curve in Fig. 13 illustrates the operational efficiency of the PEMWE system for the 1st case study over the observed 8760 h simulation period. This efficiency measurement integrates voltage efficiency, Faraday efficiency, and BoP efficiency, as detailed in Section 3.1.

Table 6
Benchmark EMS strategies.

ID	Strategy and reference	Control philosophy	MATLAB implementation summary	Relevance to benchmarking objectives
COMP	Efficiency–degradation composite optimization [52]	Non-linear/MILP optimizer balancing instantaneous stack efficiency and ageing cost via a composite objective.	Hourly solar profile as load; implement weighted objective and constraints with fmincon/intlinprog	Captures the latest co-optimization trend, directly addressing efficiency vs. longevity trade-offs.
Fuzzy	Segmented fuzzy-logic allocator [79]	Fuzzy rule-based dispatch: five power-mismatch sets dictate number of active stacks and their partial loads.	Use MATLAB fuzzy logic toolbox; adapt membership functions and rule base from 100-stack case to 4-stack.	Exemplifies intelligent, ultrafast heuristics with minimal CPU load and reduced stack cycling.
MAS	Decentralized multi-agent scheduling (MAS + MTP) [59]	Each stack is an agent solving a local LP; agents negotiate via ADMM to reach globally optimal power allocation.	Model four agents in MATLAB; they iteratively solve subproblems and update consensus on forecast power.	Demonstrates scalable, modular coordination suited to large-scale PEMWE farms and enhanced fault tolerance
RB	Threshold-based rule EMS [57]	Conventional on/off control with hysteresis: stacks switch on above an upper UF threshold and off below a lower.	Simple if–else logic using UF_{on}/UF_{off} thresholds across four stacks in a sequential loop.	Serves as the industrial baseline, illustrating classic rule-based operation and minimal algorithmic complexity.

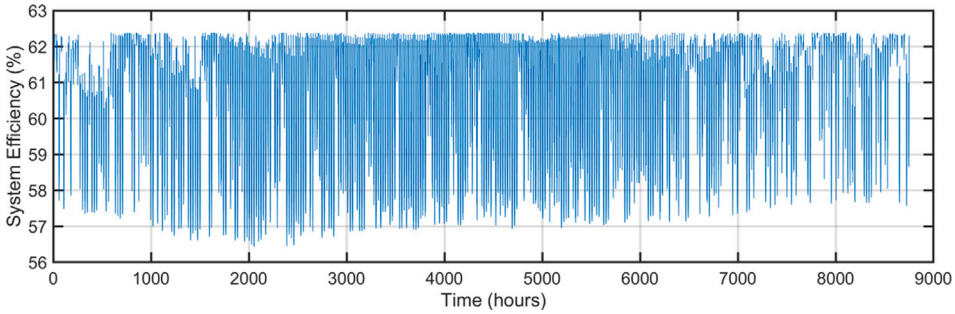

Fig. 13. System efficiency over time for PEMWE: case study 1.

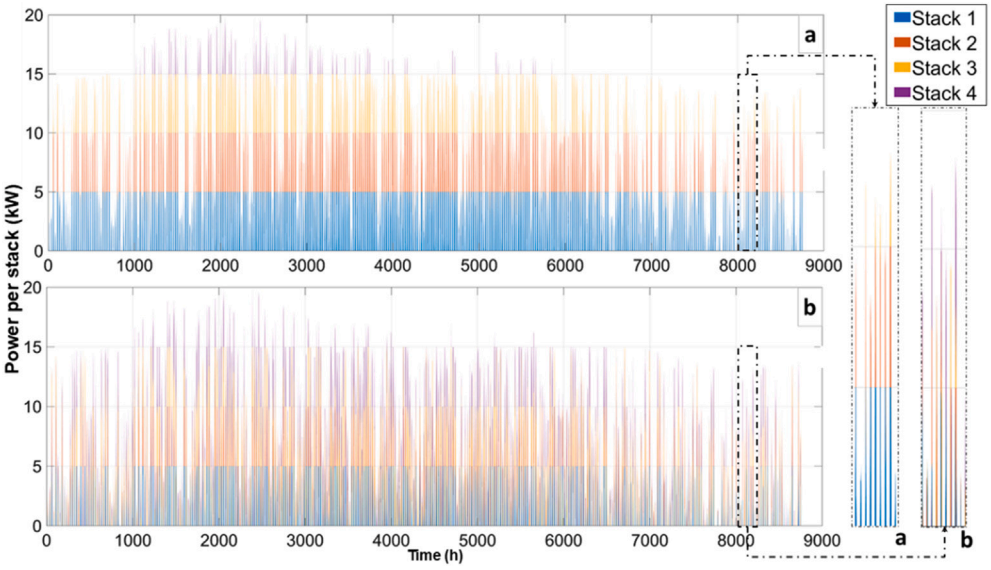

Fig. 14. Input power allocation to each stack for (a) simple rule-based EMS (b) developed EMS: 1st case study.

The efficiency generally remains consistently above 57 %, with occasional peaks approaching 63 %, reflecting effective EMS. The minor fluctuations depicted in the graph are attributed to variations in solar energy inputs, demonstrating the adaptive capability and robustness of the developed EMS. This performance highlights the success of the proposed EMS in maintaining optimal efficiency despite intermittent renewable energy supply, thereby significantly mitigating potential efficiency losses associated with fluctuating operational conditions and enhancing overall system resilience and longevity.

The comparison of input power allocation between RB and PS approaches is depicted in Fig. 14, offers a revealing insight into the efficiency and effectiveness of advanced power distribution strategies. Graphs show the allocation of power for four stacks within a PEMWE system over 8760 h.

In the simple RB strategy, power distribution is somewhat uniform but prone to sudden spikes and drops as shown in Fig. 14(a). Each stack receives power in a fixed sequence, regardless of its current efficiency or state of degradation. Despite the simplicity of this approach, it may result in inefficiencies. For example, power may continue flowing to an almost full stack, leading to increased wear and inefficiencies because of overloading. However, the PS (see Fig. 14(b)) uses an adaptive and dynamic power allocation technique which enhances the overall

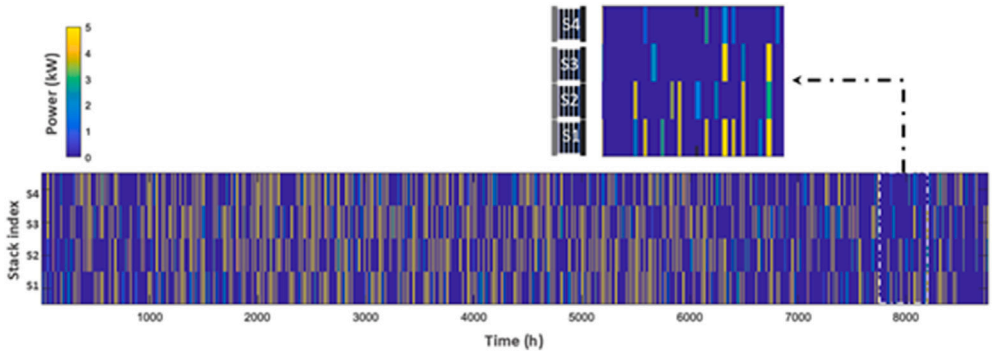

Fig. 15. Heatmap of power allocation: developed EMS.

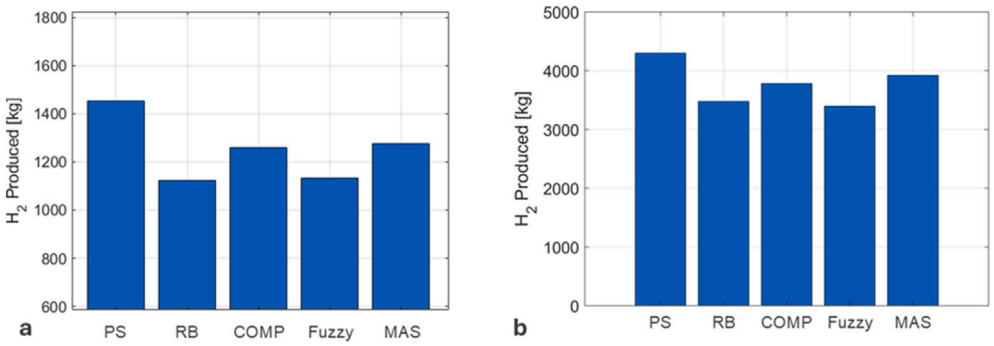

Fig. 16. Total annual hydrogen yield: (a) 1st case study and (b) 2nd case study.

performance of the system as well as maintains the overall health of each stack while improving the overall operating efficiency.

The modular PEMWE system efficiency with the PS has increased compared to linear power allocation. Specifically, simulations show that the proposed EMS achieves an average efficiency of about 62 %, approximately 5–6 % higher than that observed with the simple approach. It minimizes energy loss and lowers the chance of stack deterioration by allocating power based on real-time data and stack performance. Specifically, by avoiding prolonged high-power operation in any single stack. A regular wear and tear rate is maintained by distributing the current evenly throughout all stacks, which is essential for the system's lifetime and dependability. The designed EMS optimizes the response of the system to varying power inputs by adapting to shifting stack performance levels as well as power availability conditions.

For 1st case study, a heatmap showing the power distribution over 8760 h across four stacks based on the proposed EMS method is shown in Fig. 15. The stack index is indicated on the y-axis, while hours are displayed on the horizontal axis. Each stack can be classified according to its power allocation by its color intensity, which ranges from yellow, indicating full capacity, to dark blue, which represents no power allocation.

As shown in Fig. 15, the PS is flexible and dynamic. The EMS modifies power distribution based on stack efficiency and performance in real-time, as opposed to the RB method system that distributes power in a predetermined order. As indicated by the heatmap, a balanced power allocation rotation will guarantee that no stack ever becomes overloaded. This strategy promotes uniform degradation, enhances system reliability, and maintains higher operational efficiency by evenly distributing the load over the system's operational lifetime. The adaptive allocation is evident from the varying intensities, demonstrating how the EMS reacts to fluctuating input power and stack conditions.

Fig. 16 presents a comparative analysis of total hydrogen production across five different EMS implemented for both 1st and 2nd case studies. Fig. 16(a) illustrates the hydrogen yield for the 1st case study for each EMS over a specific representative operational period, emphasizing performance variations in a short-term or scenario-based context. The proposed EMS demonstrates the highest hydrogen production, followed by MAS, COMP, Fuzzy, and RB approaches. Fig. 16(b) shows the cumulative hydrogen production over a complete annual simulation for the 2nd case study. The developed EMS again outperforms other strategies, producing more than 4200 kg of hydrogen annually. The MAS strategy follows closely, while COMP, Fuzzy, and RB methods yield slightly lower

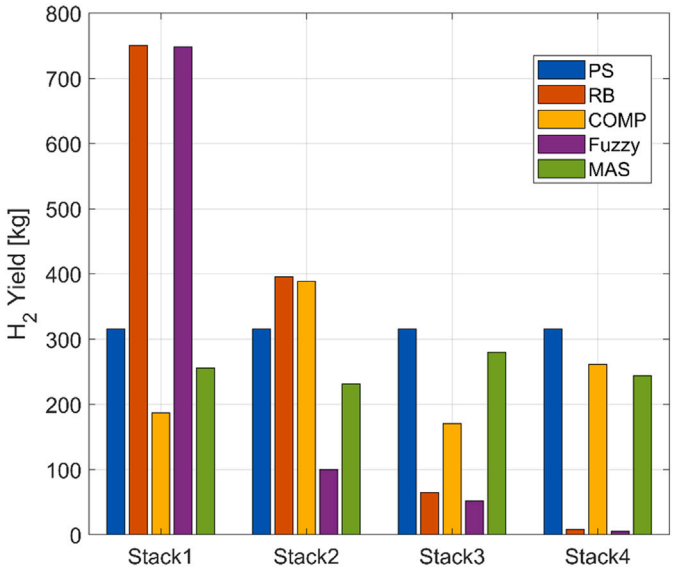

Fig. 17. Per-stack total HyPro by strategy for the 1st case study.

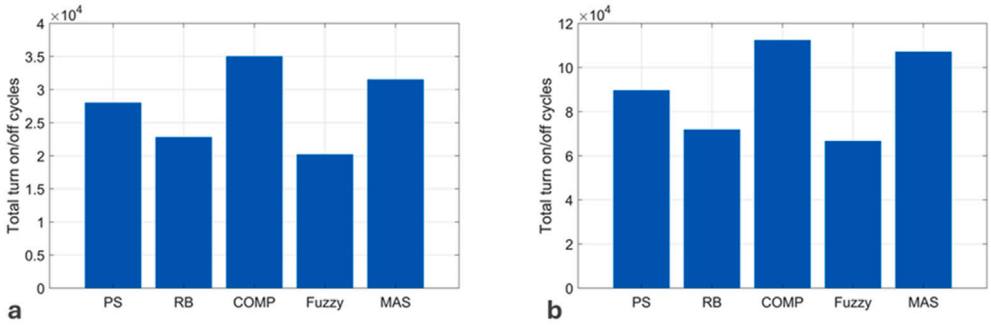

Fig. 18. Total on–off cycles over one year: (a) 1st case study and (b) 2nd case study.

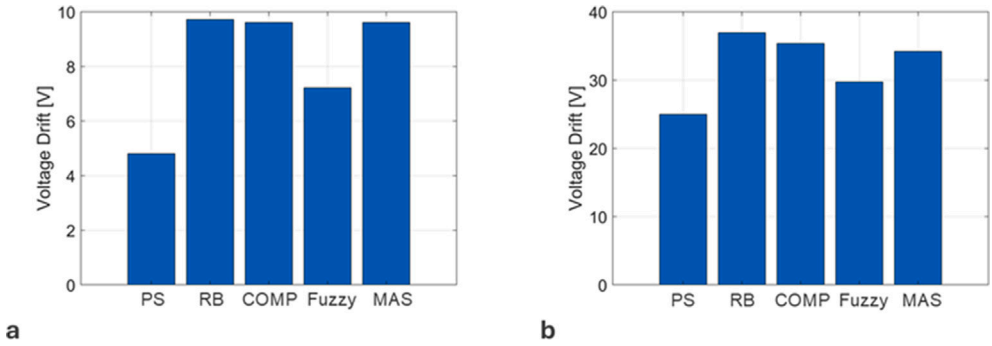

Fig. 19. Total stack degradation over one year: (a) 1st case study and (b) 2nd case study.

outputs, highlighting the trade-offs between simplicity and performance. Through dynamic stack allocation and constrained optimization, these results demonstrate the superiority of the developed EMS in maximizing hydrogen yield.

Fig. 17 illustrates the distribution of cumulative hydrogen production per stack under each of the five EMS strategies for the 1st case study. Each of the four stacks contributes approximately 32 kg to the proposed EMS, illustrating effective utilization and minimal disparity. In contrast, the RB and Fuzzy approaches heavily overload stack 1–each exceeding 740 kg–while underutilizing the remaining stacks, with yields sharply declining to near zero by stack 4. This uneven allocation reflects their lack of degradation-aware distribution logic. The COMP method shows moderate distribution, with stack 2 receiving the highest load (≈390 kg) and stack 3 the lowest (≈170 kg), suggesting partial optimization. The MAS strategy maintains more equitable allocation than the heuristic methods but still falls short of the uniformity demonstrated by the Developed EMS. As a result of these findings, it has been demonstrated that the latter is superior to the former in terms of both efficiency as well as stack longevity because of its harmonized operation, which reinforces its suitability for long-term deployment in modular electrolyzer systems.

A comparison of the total on/off cycles for both case studies using various EMS strategies can be seen in Fig. 18. For the 1st case, the COMP strategy (see Fig. 18(a)) shows the highest switching frequency (35,000 cycles) in comparison to the 2nd case study, indicating an aggressive allocation pattern sought to maximize instantaneous efficiency at the expense of stack longevity, as cycling-induced degradation may jeopardise stack longevity. Conversely, the Fuzzy logic method exhibits the lowest number of switching events (≈20,000 cycles), highlighting its capability for smoother power allocation and reduced operational stress on the stacks. There is a moderate cycle frequency with both PS and MAS strategies maintaining a balanced operational profile with an intermediate behavior.

For the 2nd case study (see Fig. 18(b)), the COMP strategy again records the highest cycling rate (≈110,000 cycles), further accentuating

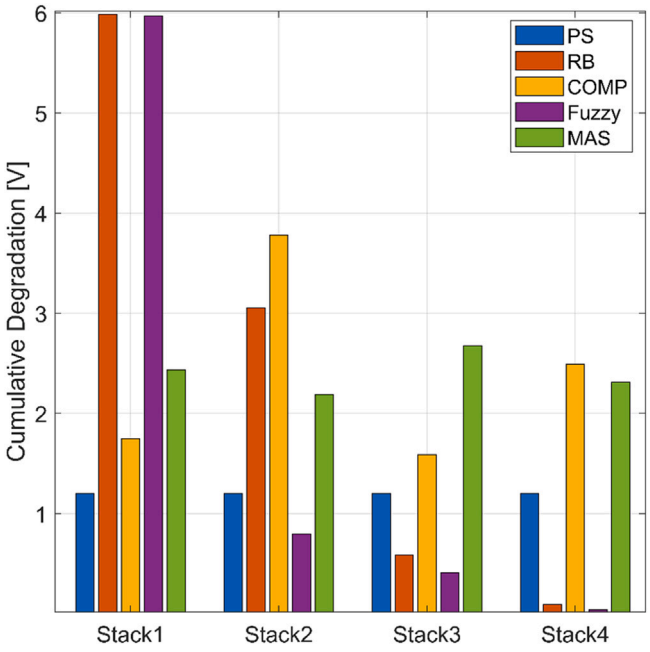

Fig. 20. Per-stack total degradation by strategy for the 1st case study.

concerns regarding long-term operational degradation. In the MAS strategy, there is also a high period of cycling (10,000 cycles), indicating frequent adjustments as a result of the decentralized negotiation process. Meanwhile, the Fuzzy logic again demonstrates the lowest cycling rate (≈60,000 cycles), validating its consistency in minimizing switching stress. In terms of cycle rate, the EMS (PS) is capable of attaining an average of 85,000 cycles during its lifetime, which reinforces its balanced

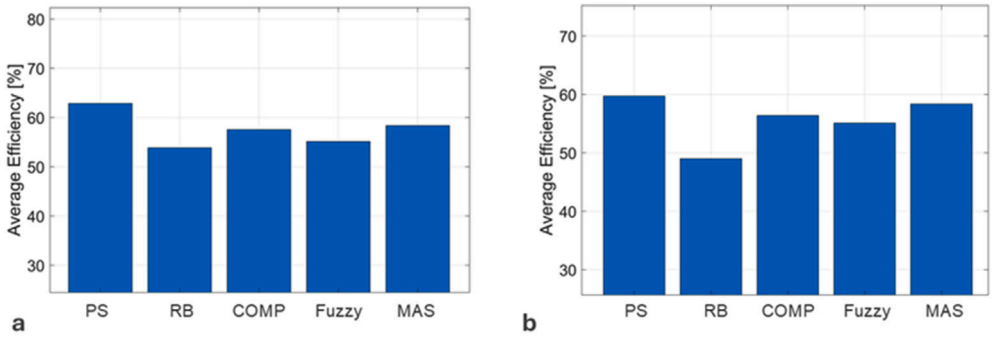

Fig. 21. Mean annual efficiency per strategy: (a) 1st case study (b) 2nd case study.

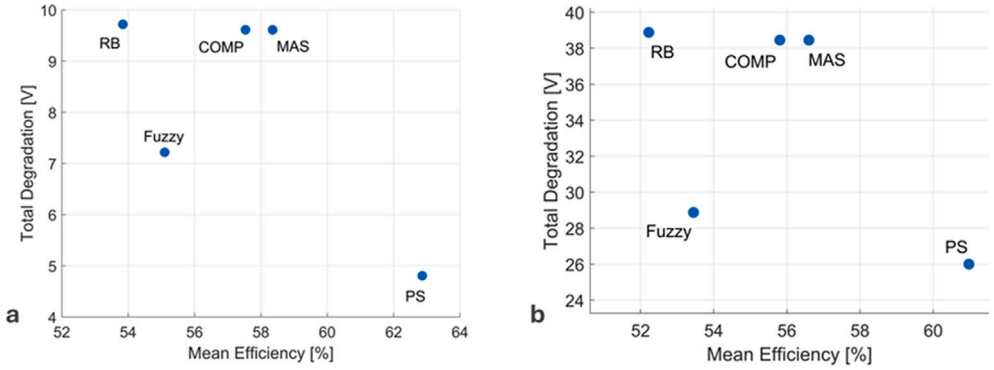

Fig. 22. Performance trade-off: efficiency vs. degradation: (a) 1st case study (b) 2nd case study.

operation, which effectively mitigates excessive switching without compromising the system's performance. Overall, these results highlight the strategic trade-offs between operational stability and efficiency, underscoring the value of employing the Developed EMS as a robust and balanced management strategy.

Fig. 19 compares the cumulative voltage drift–a proxy for stack degradation–across all strategies for both considered case studies. This figure demonstrates that the developed EMS has the lowest total voltage drift, which indicates that it is more capable of mitigating long-term degradation than the other EMSs. Specifically, for the 1st case study, (see Fig. 19(a)), the developed EMS achieves a drift below 5 V, nearly halving the degradation seen in the RB and COMP methods, both of which approach the 10 V mark. When compared to the developed approach, the Fuzzy and MAS strategies perform slightly better, but still show elevated degradation. For the 2nd case, (see Fig. 19(b)), which represents a more dynamic or stress-loaded condition, the differences are amplified: the developed EMS maintains voltage drift around 25 V, whereas RB and COMP strategies exceed 35 V. Due to this contrast, the developed EMS has the ability to distribute load uniformly and reduce stress-induced wear. Collectively, the results affirm that without integrated degradation awareness, heuristic and even some optimization-based approaches may accelerate long-term performance losses, underscoring the value of degradation-conscious energy management.

Fig. 20 illustrates the cumulative degradation experienced by each stack under the five EMS strategies for the 1st case study. The results highlight a key strength of the proposed EMS, which maintained a uniform and minimal degradation profile across all four stacks, with values remaining below 1.3 V. Stack 1 in both cases reached the imposed upper degradation cap (6 V) in both RB and Fuzzy strategies. This suggests poor load distribution and over-utilization of a single stack under these control methods. The COMP and MAS strategies performed better, yet still showed noticeable degradation disparities among stacks, indicating room for improvement in balancing long-term wear. Overall, the developed method demonstrated superior capability in mitigating degradation and ensuring more equitable stack utilization over time.

Fig. 21 presents the average annual efficiency of the five energy management strategies across two case studies. According to both Fig. 21(a) and Fig. 21(b), the developed EMS consistently produces the highest mean efficiency, exceeding 62 % for the 1st case study and around 60 % for the 2nd case study. This demonstrates its ability to provide favorable electrochemical operating conditions while allocating power across stacks equally. The COMP and MAS strategies perform moderately well, each stabilizing around 57–59 %, reflecting their capacity to adapt to dynamic conditions, albeit without explicit prioritization of efficiency over other factors. In contrast, RB and Fuzzy approaches underperform in both cases, with RB strategies exhibiting the lowest efficiency due to their rigid allocation patterns and limited responsiveness to stack performance characteristics. According to the research, combining optimization with power rotation, as in the developed EMS, yields tangible efficiency gains and justifies its position as a performance benchmark in modular PEMWE systems.

A two-dimensional comparison of the five strategies for both case studies' mean efficiency and total degradation is shown in Fig. 22. The Developed EMS (PS) for the 1st case study (see Fig. 22(a)) performs more effectively than every other EMS, offering the highest efficiency (63 %) and a low total degradation 4.8 V, indicating a balanced approach to both short-term performance and long-term health. The RB, COMP, and MAS strategies, on the other hand, show moderate efficiency values (roughly 54 %–59 %) but high degradation levels 9.6 V. Fuzzy logic approaches are notable for their relatively low degradation, but at the expense of reduced efficiency, suggesting a less-than-ideal trade-off between degradation and efficiency.

For the 2nd case study (see Fig. 22(b)), a similar trend emerges, reinforcing the superior performance of the Developed EMS (PS), which again achieves the highest efficiency (≈61 %) and notably lower degradation 26 V relative to competing strategies. It is estimated that

the RB, COMP, and MAS strategies still cluster together with high degradation levels (approximately 37–38 V) and moderate improvements in efficiency (between 54 % and 57 %). The Fuzzy logic approach again offers lower degradation compared to these three strategies, albeit accompanied by lower efficiency. In combination, both case studies indicate that the PS has the capability to consistently strike an optimal balance between efficiency maximization and degradation minimization, thereby positioning it in the most advantageous region of the performance-degradation trade-off.

5. Conclusions

For modular PEMWE units, this study proposes a nonlinear optimization-based energy management system, which can operate effectively as solar energy fluctuates. The proposed Rotary Power Allocation Strategy (RPAS) demonstrated a superior capability in balancing efficiency, degradation, and stack utilization through dynamic, real-time power allocation. Comparative evaluations against four established EMS approaches–including rule-based, fuzzy logic, composite optimization, and decentralized multi-agent scheduling–revealed that the developed method consistently achieved the highest annual efficiency (≈63 %) and hydrogen yield, while also exhibiting the lowest cumulative stack degradation across multiple case studies.

The optimized EMS significantly mitigated voltage rise, prolonged stack life, and promoted equitable utilization of all modules. Importantly, it outperformed both heuristic and partially optimized methods in adapting to variable power inputs while preserving electrochemical integrity. Achieving these improvements is particularly critical for scaling up green hydrogen production infrastructure, where lifetime performance and operational reliability have a direct impact on the economics and sustainability of systems.

In addition to technical validation using a detailed PEMWE model and solar datasets from Québec and Alberta, this work highlights the importance of integrating degradation-aware control into EMS design. The findings underscore the feasibility and necessity of applying such EMS in practical hydrogen production systems. It may be possible to explore the development of real-time hardware, the integration of dispatch signals at the grid level, and the extension to predictive and learning-based EMS frameworks in the future to achieve even greater adaptability and resilience.

CRediT authorship contribution statement

Ashkan Makhsoos: Writing – review & editing, Writing – original draft, Visualization, Validation, Software, Methodology, Investigation, Data curation, Conceptualization. **Mohsen Kandidayeni:** Writing – review & editing, Validation. **Meziane Ait Ziane:** Writing – review & editing, Validation. **Mohammadreza Moghadari:** Writing – review & editing, Data curation. **Loïc Boulon:** Writing – review & editing, Supervision, Project administration, Funding acquisition. **Bruno G. Pollet:** Writing – review & editing, Supervision.

Declaration of competing interest

The authors declare that they have no known competing financial interests or personal relationships that could have appeared to influence the work reported in this paper.

Acknowledgements

This work was supported in part by the Natural Sciences and Engineering Research Council of Canada (NSERC) (2018-06527).

Data availability

The source of the data is mentioned in the article.

References

[1] Rathor SK, Saxena D. Energy management system for smart grid: an overview and key issues. Int J Energy Res 2020;44(6):4067–109.
[2] Bekiroglu E, Esmer S. Improved energy management system for wind power-based microgrid with EV charge station. Electr Power Compon Syst 2024:1–13.
[3] Ammari C, Belatrache D, Touhami B, Makhloufi S. Sizing, optimization, control and energy management of hybrid renewable energy system–a review. Energy Built Environ 2022;3(4):399–411.
[4] Du B, Zhu S, Zhu W, Lu X, Li Y, Xie C, et al. Energy management and performance analysis of an off-grid integrated hydrogen energy utilization system. Energy Convers Manag 2024;299:117871.
[5] Makhsoos A, Kandidayeni M, Pollet BG, Boulon L. A perspective on increasing the efficiency of proton exchange membrane water electrolyzers—a review. Int J Hydrogen Energy 2023;48(41):15341–70. https://doi.org/10.1016/j.ijhydene.2023.01.048
[6] Moghadari M, Kandidayeni M, Boulon L, Chaoui H. Hydrogen minimization of a hybrid multi-stack fuel cell vehicle using an optimization-based strategy. In: 2021 IEEE vehicle power and propulsion conference (VPPC); IEEE; 2021. p. 1–5.
[7] Su W, Li Q, Zheng W, Han Y, Yu Z, Bai Z, et al. Enhancing wind-solar hybrid hydrogen production through multi-state electrolyzer management and complementary energy optimization. Energy Rep 2024;11:1774–86.
[8] Nezhad MA. Coordination of demand side management and aqua electrolyzer based on unabsorbed electricity for improvement of energy efficiency in energy optimization programming under renewable uncertainties. Process Integr Optim Sustain 2024;8(4):1107–17. https://doi.org/10.1007/s41660-024-00420-8
[9] Colangelo G, Spirto G, Milanese M, de Risi A. Hydrogen production from renewable energy resources: a case study. Energy Convers Manag 2024;311:118532.
[10] Lopez VAM, Ziar H, Haverkort JW, Zeman M, Isabella O. Dynamic operation of water electrolyzers: a review for applications in photovoltaic systems integration. Renew Sustain Energy Rev 2023;182:113407. https://doi.org/10.1016/j.rser.2023.113407
[11] Makhsoos A, Kandidayeni M, Boulon L, Pollet BG, Kelouwani S. Evaluation of high-efficiency hydrogen production from solar energy using artificial neural network at the Université du Québec á Trois-Rivières. In: 2022 IEEE vehicle power and propulsion conference (VPPC); 2022. p. 1–6. https://doi.org/10.1109/VPPC55846.2022.10003314
[12] Thijs B, Houlleberghs M, Hollevoet L, Heremans G, Rongé J, Martens JA. Hydrogen, fueling the future: introduction to hydrogen production and storage techniques. Hydrogen Storage Sustain 2:159–94.
[13] Bareiß K, de la Rua C, Möckl M, Hamacher T. Life cycle assessment of hydrogen from proton exchange membrane water electrolysis in future energy systems. Appl Energy 2019;237:862–72.
[14] Liu J, et al. Efficient and stable proton exchange membrane water electrolysis enabled by stress optimization. ACS Central Sci 2024;10(4):852–9.
[15] Sharifzadeh M, Cooper N, van't Noordende H, Shah N. Operational strategies and integrated design for producing green hydrogen from wind electricity. Int J Hydrogen Energy 2024;64:650–75. https://doi.org/10.1016/j.ijhydene.2024.03.237
[16] Lange H, Klose A, Beisswenger L, Erdmann D, Urbas L. Modularization approach for large-scale electrolysis systems: a review. Sustain Energy Fuels 2024;8(6):1208–24. https://doi.org/10.1039/D3SE01588B
[17] Chatenet M, Pollet BG, Dekel DR, Dionigi F, Deseure J, Millet P, et al. Water electrolysis: from textbook knowledge to the latest scientific strategies and industrial developments. Chem Soc Rev 2022;51(11):4583–762.
[18] Schwarze K, Geißler T, Nimtz M, Blumentritt R. Demonstration and scale-up of high-temperature electrolysis systems. Fuel Cells 2023;23(6):492–500. https://doi.org/10.1002/fuce.202300059
[19] Huang D, Zhong Z, Ai X, Hu K, Xiong B, Wen Q, et al. Size design strategy for scaling up alkaline water electrolysis stack integrated with renewable energy source: a multiphysics modeling approach. Energy Convers Manag 2024;300:117955.
[20] Schmidt O, Gambhir A, Staffell I, Hawkes A, Nelson J, Few S. Future cost and performance of water electrolysis: an expert elicitation study. Int J Hydrogen Energy 2017;42(52):30470–92. https://doi.org/10.1016/j.ijhydene.2017.10.045
[21] Chandrasekar A, Flynn D, Syron E. Operational challenges for low and high temperature electrolyzers exploiting curtailed wind energy for hydrogen production. Int J Hydrogen Energy 2021;46(57):28900–11. https://doi.org/10.1016/j.ijhydene.2020.12.217
[22] Sharifzadeh M, Garcia MC, Shah N. Supply chain network design and operation: systematic decision-making for centralized, distributed, and mobile biofuel production using mixed integer linear programming (MILP) under uncertainty. Biomass Bioenergy 2015;81:401–14. https://doi.org/10.1016/j.biombioe.2015.07.026
[23] Salman BA. Balancing and frequency control of power systems in presence of wind farms and utility-scale power-to-hydrogen plants. 2022.
[24] Alirahmi SM, Assareh E, Arabkoohsar A, Yu H, Hosseini SM, Wang X. Development and multi-criteria optimization of a solar thermal power plant integrated with PEM electrolyzer and thermoelectric generator. Int J Hydrogen Energy 2022;47(57):23919–34. https://doi.org/10.1016/j.ijhydene.2022.05.196
[25] Shiroudi A, Taklimi SRH, Jafari N. Case study: technical assessment of the efficiency optimization in direct connected PV-electrolysis system at Taleghan-Iran. Fuel Cells 2011;4:1150.
[26] Zhang F, Wang B, Gong Z, Zhang X, Qin Z, Jiao K. Development of photovoltaic-electrolyzer-fuel cell system for hydrogen production and power generation. Energy 2023;263:125566. https://doi.org/10.1016/j.energy.2022.125566
[27] Ziogou C, Ipsakis D, Seferlis P, Bezergianni S, Papadopoulou S, Voutetakis S. Optimal production of renewable hydrogen based on an efficient energy management strategy. Energy 2013;55:58–67. https://doi.org/10.1016/j.energy.2013.03.017

[28] Jin J, Wang Z, Chen Y, Xie C, Wu F, Wen Y. Modeling and energy management strategy of hybrid energy storage in islanded DC micro-grid. Electr Eng 2024. https://doi.org/10.1007/s00202-024-02376-x
[29] Guilbert D, Sorbera D, Vitale G. A stacked interleaved DC-DC buck converter for proton exchange membrane electrolyzer applications: design and experimental validation. Int J Hydrogen Energy 2020;45(1):64–79. https://doi.org/10.1016/j.ijhydene.2019.10.238
[30] Shakibi H, Faal MY, Assareh E, Agarwal N, Yari M, Latifi SA, et al. Design and multi-objective optimization of a multi-generation system based on PEM electrolyzer, RO unit, absorption cooling system, and ORC utilizing machine learning approaches; a case study of Australia. Energy 2023;278:127796.
[31] Liu X. Optimization method for capacity configuration and power allocation of electrolyzer array in off-grid integrated energy system. Heliyon 2024.
[32] Nguyen KM, Phan LV, Nguyen DD, Nguyen TD. A comprehensive technical analysis on optimal sizing and operating strategy for large-scale direct coupled PV–electrolyser systems, considering PV system faults, degradation and partial shading conditions. Int J Hydrogen Energy 2024;59:492–506. https://doi.org/10.1016/j.ijhydene.2024.02.043
[33] Su Z, Liu J, Li P, Liang C. Study of the durability of membrane electrode assemblies in various accelerated stress tests for proton-exchange membrane water electrolysis. Materials (Basel) 2024;17(6). https://doi.org/10.3390/ma17061331
[34] Siracusano S, Trocino S, Briguglio N, Pantò F, Aricò A. Analysis of performance degradation during steady-state and load-thermal cycles of proton exchange membrane water electrolysis cells. J Power Sources 2020;468:228390. https://doi.org/10.1016/j.jpowsour.2020.228390
[35] Frensch SH, Fouda-Onana F, Serre G, Thoby D, Araya SS, Kær SK. Influence of the operation mode on PEM water electrolysis degradation. Int J Hydrogen Energy 2019;44(57):29889–98. https://doi.org/10.1016/j.ijhydene.2019.09.169
[36] Rakousky C, Reimer U, Wippermann K, Carmo M, Lueke W, Stolten D. An analysis of degradation phenomena in polymer electrolyte membrane water electrolysis. J Power Sources 2016;326:120–28. https://doi.org/10.1016/j.jpowsour.2016.06.082
[37] Alia SM, Stariha S, Borup RL. Electrolyzer durability at low catalyst loading and with dynamic operation. J Electrochem Soc 2019;166(15):F1164. https://doi.org/10.1149/2.0231915jes
[38] Babic U, Tarik M, Schmidt TJ, Gubler L. Understanding the effects of material properties and operating conditions on component aging in polymer electrolyte water electrolyzers. J Power Sources 2020;451:227778. https://doi.org/10.1016/j.jpowsour.2020.227778
[39] Kumar K, Alam M, Dutta V. Energy management strategy for integration of fuel cell-electrolyzer technologies in microgrid. Int J Hydrogen Energy 2021;46(68):33738–55. https://doi.org/10.1016/j.ijhydene.2021.07.203
[40] Wang Y, Advani SG, Prasad AK. A comparison of rule-based and model predictive controller-based power management strategies for fuel cell/battery hybrid vehicles considering degradation. Int J Hydrogen Energy 2020;45(58):33948–56. https://doi.org/10.1016/j.ijhydene.2020.09.030
[41] Ziogou C, Dimitrios I, Seferlis P, Bezergianni S, Papadopoulou S, Voutetakis S. Optimal production of renewable hydrogen based on an efficient energy management strategy. Energy 2013;55:58–67. https://doi.org/10.1016/j.energy.2013.03.017
[42] Majumdar A, Haas M, Elliot I, Nazari S. Control and control-oriented modeling of PEM water electrolyzers: a review. Int J Hydrogen Energy 2023;48(79):30621–41.
[43] Benmehel A, Chabab S, Nascimento AD, Chepy M, Kousksou T. PEM water electrolyzer modeling: issues and reflections. Energy Convers Manag 2024;X:100738.
[44] Hernández-Gómez A, Ramirez V, Guilbert D. Investigation of PEM electrolyzer modeling: electrical domain, efficiency, and specific energy consumption. Int J Hydrogen Energy 2020;45(29):14625–39. https://doi.org/10.1016/j.ijhydene.2020.03.195
[45] Hernández-Gómez A, Ramirez V, Guilbert D, Saldivar B. Cell voltage static-dynamic modeling of a PEM electrolyzer based on adaptive parameters: development and experimental validation. Renew Energy 2021;163:1508–22.
[46] Zheng Y, Huang C, Tan J, You S, Zong Y, Træholt C. Off-grid wind/hydrogen systems with multi-electrolyzers: optimized operational strategies. Energy Convers Manag 2023;295:117622.
[47] Li J. A multi-stack power-to-hydrogen load control framework for the power factor-constrained integration in volatile peak shaving conditions. 2023. arXiv:2301.09578
[48] Han P, Xu X, Wang H, Yan Z. Operational efficiency enhancement of multi-stack proton exchange membrane electrolyzer systems with power-temperature adaptive control. Trans China Electrotech Soc 2023.
[49] Guilbert D, Vitale G. Improved hydrogen-production-based power management control of a wind turbine conversion system coupled with multistack proton exchange membrane electrolyzers. Energies 2020;13(5):1239.
[50] Tully Z, Starke G, Johnson K, King J. An investigation of heuristic control strategies for multi-electrolyzer wind-hydrogen systems considering degradation. In: 2023 IEEE conference on control technology and applications (CCTA); IEEE; 2023. p. 817–22.
[51] Lu X, Du B, Zhou S, Zhu W, Li Y, Yang Y, et al. Optimization of power allocation for wind-hydrogen system multi-stack PEM water electrolyzer considering degradation conditions. Int J Hydrogen Energy 2023;48(15):5850–72.
[52] Zheng W, Lv B, Shao Z, Zhang B, Liu Z, Sun J, et al. Optimization of power allocation for the multi-stack PEMEC system considering energy efficiency and degradation. Int J Hydrogen Energy 2024;53:1210–25.
[53] Zhang H, Yuan T. Optimization and economic evaluation of a PEM electrolysis system considering its degradation in variable-power operations. Appl Energy 2022;324:119760.
[54] Cheng K, He S, Hu B. Power adaptive control strategy for multi-stack PEM photovoltaic hydrogen systems considering electrolysis unit efficiency and hydrogen production rate. Sustain Energy Technol Assess 2025;75:104200.
[55] Varela C, Mostafa M, Zondervan E. Modeling alkaline water electrolysis for power-to-x applications: a scheduling approach. Int J Hydrogen Energy 2021;46(14):9303–13.
[56] Zhao Y, Zhu Z, Tang S, Guo Y, Sun H. Electrolyzer array alternate control strategy considering wind power prediction. Energy Rep 2022;8:223–32.
[57] Fang R, Liang Y. Control strategy of electrolyzer in a wind-hydrogen system considering the constraints of switching times. Int J Hydrogen Energy 2019;44(46):25104–11.
[58] Muyeen SM, Takahashi R, Tamura J. Electrolyzer switching strategy for hydrogen generation from variable speed wind generator. Electr Power Syst Res 2011;81(5):1171–79. https://doi.org/10.1016/j.epsr.2011.01.005
[59] Henkel V, Kilthau M, Gehlhoff F, Wagner L, Fay A. Cost optimized scheduling in modular electrolysis plants. In: 2024 IEEE international conference on industrial technology (ICIT); IEEE; 2024. p. 1–8.
[60] Parache F, Schneider H, Turpin C, Richet N, Debellemanière O, Bru É, et al. Impact of power converter current ripple on the degradation of PEM electrolyzer performances. Membranes 2022;12(2):109.
[61] Requena-Leal I, Fernández-Marchante CM, Lobato J, Rodrigo MA. Towards a more sustainable hydrogen energy production: evaluating the use of different sources of water for chloralkaline electrolyzers. Renew Energy 2024;233:121137. https://doi.org/10.1016/j.renene.2024.121137
[62] Abomazid AM, El-Taweel NA, Farag HEZ. Novel analytical approach for parameters identification of PEM electrolyzer. IEEE Trans Ind Inf 2022;18(9):5870–81. https://doi.org/10.1109/TII.2021.3132941
[63] Makhsoos A, Kandidayeni M, Ziane MA, Boulon L, Pollet BG. Model benchmarking for PEM water electrolyzer for energy management purposes. Energy Convers Manag 2025;323:119203. https://doi.org/10.1016/j.enconman.2024.119203
[64] Dobos AP. PVWatts version 5 manual. 2014. https://www.osti.gov/biblio/1158421
[65] AESO. Historical generation data (CSD). 2024. https://www.aeso.ca/market/market-and-system-reporting/data-requests/historical-generation-data
[66] Sezer N, Bayhan S, Fesli U, Sanfilippo A. A comprehensive review of the state-of-the-art of proton exchange membrane water electrolysis. Mater Sci Energy Technol 2025;8:44–65. https://doi.org/10.1016/j.mset.2024.07.006
[67] Lu X, Du B, Zhou S, Zhu W, Li Y, Yang Y, et al. Optimization of power allocation for wind-hydrogen system multi-stack PEM water electrolyzer considering degradation conditions. Int J Hydrogen Energy 2023;48(15):5850–72.
[68] Chidziva S, Malinowski M, Bladergroen B, Pasupathi S, Lototskyy M. PEM electrolysis system performance and system safety integration. Nat Gas Ind B 2020;22:2.
[69] Landin NK, Windom BC. Evaluating the efficiency of a proton exchange membrane green hydrogen generation system using balance of plant modeling. Int J Hydrogen Energy 2024;57:1273–85. https://doi.org/10.1016/j.ijhydene.2024.01.128
[70] Makhsoos A, Kandidayeni M, Boulon L, Pollet BG. A comparative analysis of single and modular proton exchange membrane water electrolyzers for green hydrogen production - a case study in Trois-Rivières. Energy 2023;282:128911. https://doi.org/10.1016/j.energy.2023.128911
[71] Kim S, Hyun K, Kwon Y. Effects of voltage stress conditions on degradation of iridium-based catalysts occurring during high-frequency operation of PEM water electrolysis. Chem Eng J 2024;496:154288. https://doi.org/10.1016/j.cej.2024.154288
[72] Wallnöfer-Ogris E, Grimmer I, Ranz M, Höglinger M, Kartusch S, Rauh J, et al. A review on understanding and identifying degradation mechanisms in PEM water electrolysis cells: insights for stack application, development, and research. Int J Hydrogen Energy 2024;65:381–97.
[73] Papakonstantinou G, Algara-Siller G, Teschner D, Vidaković-Koch T, Schlögl R, Sundmacher K. Degradation study of a proton exchange membrane water electrolyzer under dynamic operation conditions. Appl Energy 2020;280:115911.
[74] Zeng Z, Ouimet R, Bonville L, Niedzwiecki A, Capuano C, Ayers K, et al. Degradation mechanisms in advanced meas for PEM water electrolyzers fabricated by reactive spray deposition technology. J Electrochem Soc 2022;169(5):054536.
[75] Boyd S, Vandenberghe L. Convex optimization. Cambridge University Press; 2004.
[76] Bertsekas DP. Nonlinear programming. J Oper Res Soc 1997;48(3):334.
[77] MATLAB. Optimization toolbox™ user's guide, Natick, MA, USA. 2023.
[78] Wright SJ. Numerical optimization. 2006.
[79] Hong Z, Wei Z, Han X. Optimization scheduling control strategy of wind-hydrogen system considering hydrogen production efficiency. J Energy Storage 2022;47:103609.